Location of Managed Realignment Sites in Scheldt Estuary has Opposing Effect on Salt Intrusion

Master Thesis, CEM

(Civil Engineering & Management)

By Marnix Riepen

23-09-2024

Graduation committee:

dr. ir. B. W. (Bas) Borsje	-	Chair (UT)
J. (Jesse) Bootsma MSc	-	Daily supervisor (UT)
J. (Joris) Vanlede	-	Supervisor (Flanders Hydraulics)

Faculty of Engineering Technology, Water Engineering and management, University of Twente.

Preface

Over the past eight months, I have gained some experience in researching a topic that remains largely unexplored. Salinity, often regarded as the lesser-known counterpart to other processes, such as water safety, sediment transport, etc., has traditionally received less attention due to its lack of immediate impact on human life. However, with rising sea levels and increasing freshwater scarcity, its significance is growing. This paper presents the knowledge I have gathered throughout this research. I was able to gather this information by the help of my supervisors. I would like to express my sincere gratitude to Jesse Bootsma MSc, my daily supervisor from the University of Twente, who consistently made time to answer my numerous questions, and provided invaluable guidance throughout this process. I would also like to thank dr. ir. Bas Borsje for overseeing the progress and for answering the practical questions related to the graduation.

Additionally, I would like to thank my supervisor at Flanders Hydraulics, Joris Vanlede. Throughout the eight months, we held regular meetings, and I had the opportunity to visit Flanders Hydraulics twice for in-depth discussions with him and several colleagues. These visits provided a valuable opportunity to assess whether my work met the standards of a research institute and to gain insights from experienced researchers with extensive expertise in modeling. An extra special mention goes to him for taking the time to discuss various topics with me, even during his holiday. I am incredibly grateful for his support.

Lastly, I want to express my gratitude to everyone who supported me throughout this challenging period, filled with highs and lows. To my girlfriend, thank you for accompanying me on a trip to the Scheldt estuary, patiently listening to all my “boring” facts, and exploring the managed realignment sites that would be inundated in the specific scenarios. To my friends, who studied alongside me so I would not be alone, brought me snacks and coffee, and provided for some needed distraction, your company meant a lot. And to my family, thank you for standing by me through the harsh and sad moments and offering your unconditional support.

In this paper, the following AI tools were used: Grammarly, ChatGPT-4, ChatGPT-3, Copilot, and the built-in spelling corrector in Word. These tools were used only to enhance the language and check spelling. For example, I initially wrote: “This is an example for to show the use of the AI tools in this paper.” After requesting a rewrite, ChatGPT provided: “Here is an example that illustrates the use of AI tools in this paper.” The final version became: “Here is an example that shows the use of AI tools in this paper.”

I hope you will enjoy reading this paper.

Sincerely,

Marnix

Enschede, September 2024

Table of Contents

Abstract

This paper explores the effects of Managed Realignment Sites (MRS) on salt intrusion within the Scheldt Estuary. Estuaries, such as the Scheldt, are environments where freshwater and saltwater mix, and their salinity distribution is influenced by various factors, including tidal forces and river discharge. The process-based numerical model 2D (depth average) in this paper was modified to incorporate MRS locations determined by two pre-existing projects ("Dubbele Dijken" and "Sigmaplan"). A total of five scenarios were simulated: (1) a base scenario without any MRS open into the model, (2) a scenario where all MRS are open, (3) a scenario with only the MRS near the estuary's mouth open up to the Hedwige MRS, (4) a scenario where only the upstream MRS beyond the Hedwige MRS are open, and (5) a scenario where only the MRS connected to the Hedwige MRS, along with the Hedwige MRS itself, are open. The results indicate an impact on salt intrusion patterns: MRS situated near the estuary's mouth (3) led to a reduction in the average salt intrusion length (800 m) of 29 days, whereas upstream MRS (4) contribute to an increase in salt intrusion length (1700 m). Furthermore, when analyzing the average salinity along the estuary, a S-curve emerges. In the scenario where the upstream MRS are open (4), the salinity decreases near the estuary's mouth (min -0.1 psu) and then increases further upstream (max 0.6 psu). Conversely, in the scenario where the MRS near the mouth are open (3), the salinity increases close to the mouth (0.4 psu) and decreases further upstream (min -1.8 psu). The scenario with all MRS open resulted in a combined effects of scenarios 3, 4, and 5. The scenario with the enlarged Hedwige MRS (scenario 5) shows changes of less than 0.1 psu. The tidal prism exhibits a comparable pattern. The results are consistent and align with existing literature, indicating that the findings can be considered robust. Given the growing importance of sustainable strategies in estuarine management, these findings provide initial insights into the effects of MRS in affecting estuarine salinity, highlighting the need for further research in this area to inform future realignment and restoration projects.

Introduction

Estuaries are coastal zones where freshwater from rivers meets and mixes with saltwater from the ocean, creating unique and dynamic environments that support diverse ecosystems (Pritchard, 1967). The mixing length of salt in an estuary, quantified for instance by salt intrusion length (Savenije, 2005), is influenced by various factors such as river discharge, tidal forces, and cross-sectional area, which collectively affect the extent and nature of saltwater penetration into the estuary (Hendrickx, et al., 2023). Salt intrusion has significant implications for both the natural environment and human activities, particularly in relation to freshwater availability for drinking water, agriculture, and industry. This can cause for enormous economic losses (Mondal, et al., 2023). The increasing impact of climate change, including sea-level rise and altered precipitation patterns, can aggravates salt intrusion, posing challenges for the estuarine ecosystems (Raltson & Geyer, 2019). Due to these challenges, estuarine regions are constantly a subject to changes. These changes involve channel deepening, embankment construction for flood protection, and the reclamation of intertidal areas for purposes such as agriculture. However, this last-mentioned practice has become less common in certain parts of the world than it once was. Nowadays conservation and restoration of intertidal flats and marshes along estuaries is gaining ground as a sustainable strategy for flood defense (e.g. living dikes experiments in the DeltaFlume (Nesvarova, 2024). In the U.K. already 50 different sites are completed and there are plans to realign 10% of the English and Welsh coasts (Bennet, et al., 2020). The function of the realignment sites is for flood defense, new intertidal habitats or a combination of those. However, the influence of salt intrusion is often overlooked in these decisions, and the impact of intertidal areas on salt intrusion remains little understood. The following section will review the existing research on how intertidal areas affect salt intrusion.

Impact of intertidal area on salt intrusion in an estuary

Recent research highlights the significant impact of intertidal zones on salt intrusion within estuaries, thereby affecting freshwater availability (Geyer et al., 2020; Zhou et al., 2021; Siemes et al., 2023). Studies have demonstrated that tidal flats can reduce salt intrusion (Lyu & Zhu, 2019)). However, other findings suggest their influence might be negligible or could even increase salt intrusion (Siemes et al., 2023). A recent study by Hendrickx and Pearson (2023) examined the effect of intertidal areas on salt intrusion across different estuary types. The study demonstrated that in well-mixed estuaries, the expansion of intertidal areas facilitates the influx of saline water over the flats, thereby enhancing salt intrusion. These findings were based on an idealized schematization, where intertidal flats were added along the entire length of the estuary and connected to the coast. In contrast, Siemes et al., research used a back-barrier model, which separates the intertidal area from the coast, meaning all salt transport occurs through the main channel. While both studies agree that salt intrusion increases with intertidal area in well-mixed estuaries, the mechanism proposed by Hendrickx cannot explain the increase observed in Siemes model. This raises important questions about how salt intrusion behaves in more realistic models and how the precise location of intertidal zones may influence salt intrusion within the estuary.

Position of the intertidal areas

In the previous section, only idealized schematizations of intertidal areas were examined in relation to salinity. However, more realistic studies have been conducted that focus on intertidal areas, not specifically on salinity, but on hydrodynamics in general.

The position of an intertidal area and its storage volume relative to the local tidal prism determine both the intensity and extent of tidal hydrodynamic effects along the estuary (Stark et al., 2017). Stark et al. also found that intertidal areas located in the main channel (mid-channel flats / shoals) of

the estuary have varying influences depending on their elevation. When these areas are around mean sea level (MSL) or just above, ebb dominance is enhanced, while flood dominance increases if the intertidal areas are situated lower in the tidal frame. Intertidal areas that function as side basins to the main estuarine channel reduce both upstream and downstream flood dominance, where flood dominance typically peaks. Additionally, increasing intertidal storage volume in the upstream part of an estuary can decrease the total tidal prism, while adding storage volume downstream has the opposite effect. Similarly, Pontee (2015), found that large realignment sites near the mouth of an estuary have the potential to raise water levels throughout the estuary. A study by Weisscher et al. (2022), observed similar processes in transitional polders, noting that adding an upstream polder capable of flooding significantly reduces the tidal range, while adding a downstream polder slightly increases it. In conclusion, the position and elevation of an intertidal flat significantly influences estuarine hydrodynamics.

Research questions

As mentioned in the introduction, the inconsistency of height, position, resolution, idealized versions in existing studies raises important questions about the role of managed realignment sites (MRS) about the role of salt intrusion in the estuary. The objective of this paper is to investigate how the location of managed realignment sites affects the length of salt intrusion in a well-mixed estuary. The focus is on examining salt intrusion dynamics under current, real-life conditions at the estuary scale. This goal will be achieved by addressing the following research questions:

1. How do managed realignment sites affect the salt intrusion length in a well-mixed estuary?
2. What is the relation between the location/position of the managed realignment sites compared to the salt intrusion length?
3. How do the results of the process-based numerical model 2D (depth average) compare with existing literature?

The research questions outlined above are investigated using the existing Delft3D FM NeVla model, which was calibrated and validated by Deltares (Tiessen et al., 2016). The model was modified by incorporating the MRS, and then run for 365 days. The Scheldt estuary was selected as the study area due to its low discharge, the presence of intertidal area, the realized MRS Hedwige in 2022 and well-mixed characteristics.

Study Area

The Scheldt Estuary is a macrotidal estuary in Western Europe, located in Belgium and the Netherlands, about 100km west of Brussels and 50km north of Antwerp (Figure 1) (Braeckel, Vandervoorde, & Bergh, 2008). The Scheldt Estuary has undergone significant changes in its morphology and ecology due to human interventions since the early Middle Ages. People started to reclaim tidal marshes for agriculture and built dikes to protect themselves from storm surges in the 10th century. Several floods in the 14th to 16th century altered the shape of the estuary. The shipping activities increased in the 19th century, which required several deepening projects of the estuary. The industrial and urban development in the mid-20th century also had a major impact on the estuary. Its total surface area decreased by 16% in the last century (Meire, et al., 2005), and the Western Scheldt lost 15.000 ha of its area and has become 10.5 km shorter since 1800. The habitats in the Western Scheldt also changed, with a decline of low dynamic areas like mud flats and shallow water, and an increase of high dynamic areas, such as deep water and sand flats. (Interreg North Sea Region IMMERSE) The estuary receives freshwater from three sources: the Scheldt River from

Antwerp, and two canals—the Gent-Terneuzen Canal and the Bathse Spuikanaal. The freshwater flow at Schelle fluctuates between 30 and 300 m³/s, with a long-term average of approximately 120 m³/s. The estuary experiences a semi-diurnal tide, with an average tidal range of about 3.7 m at the mouth of the Western Scheldt (Vlissingen). This tidal range increases landward, reaching approximately 5.4 m at Tielrode (~100 km from the mouth), before decreasing upstream to about 2.6 m at Melle (~150 km from the mouth) (Wang et al., 2019).

The classification of the Scheldt estuary is discussed in the context of estuarine types. Multiple studies (e.g. (Meire, et al., 2005) (Vriend, et al., 2011)) suggest that the Scheldt is a well-mixed estuary, indicating a large tidal range compared to river discharge.

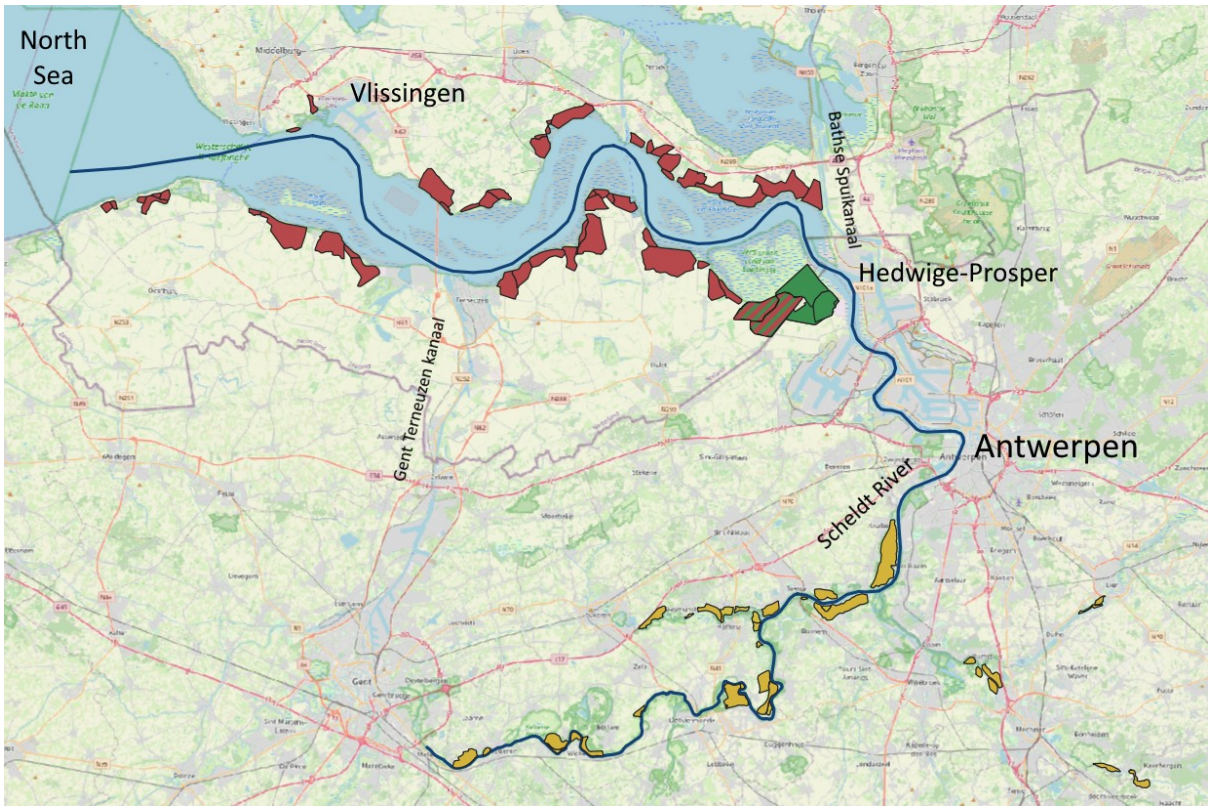

Figure 1 Map of the Scheldt Estuary highlighting key areas: the Mouth (red), Enlarged Hedwige (green), and Upstream scenarios (yellow). The blue line represents the main channel, along which data is collected every 500 meters. This line is also used to mark the observation cross sections at 5000-meter intervals.

Method

This section first discusses the model that is utilized and its configuration. Following this, the selected MRS are introduced, along with the rationale behind their selection. Afterwards, the specific scenarios simulated for this study are outlined. Lastly, the method of presenting and analyzing the model's results is explained.

Model

To address the research questions, process-based numerical modeling was selected. In this study, the Delft3D FM NeVla model for the Scheldt estuary, made and validated by Tiessen et al., (2016) is employed. Delft3D NeVla is derived from the original NeVla model which was developed and calibrated at Flanders Hydraulics as a 3D model in SIMONA-TRIWAQ (Vanlede et al., 2015). The model accurately reproduces observed water levels and flow velocities at various points within the estuary, and the results are comparable to those produced by earlier version called the Delft3D-NeVla model. The scenario runs were performed on a supercomputer (Snellius), with each Delft3D Flexible Mesh simulation running in parallel on 32 cores. Execution times of a whole year were around 5 full days.

Hydrodynamics

The Delft3D FM solves shallow water equations (depth-average in this case). These equations are derived from the Navier-Stokes equations for incompressible free surface flow. The depth is assumed to be much smaller than the horizontal length scale, validating the shallow water assumption. Consequently, the vertical momentum equation reduces to the hydrostatic pressure relation, implying that vertical accelerations are negligible compared to gravitational acceleration. Furthermore, the Navier Stokes equations is solved with the Boussinesq assumptions which imply that the variable density effects are considered only in the pressure term. The exact formula and hydrodynamic processes can be found in the manual of Delft3D FM. (Deltares , 2024).

Salinity

The salinity in the model is calculated with a transport formula including three processes: advection, diffusion and sources/sinks. The specific details can be found in the manual of Delft3D FM (Deltares , 2024). The dispersion and viscosity are set to 1 m^2/s.

Salt intrusion can be quantitatively described by the salt intrusion length, commonly defined as the distance from the mouth of the estuary to the point where the maximum salinity has decreased to 1 psu. This approach will be applied in this paper as well. In the model, salt intrusion is tracked using observation points placed along the main channel at 500-meter intervals from the estuary's mouth, see Figure 1. Since the salinity data is extracted discretely from the hydrodynamic model's numerical grid, linear interpolation between data points is used to determine the salt intrusion length.

Grid

The grid of the model is a combination of regular grid and irregular grid. Where the irregular grid is an adaption of the existing model to add the new managed realignment sites to the grid. There are some parts of the original grid that were irregular to be able to lower the total active grid cells from 250.000 to 170.000. The added realignment sites included lead to a total of 289.000 active grid cells, see Figure 2. An extensive implementation of the MRS in the grid can be found in Appendix B.

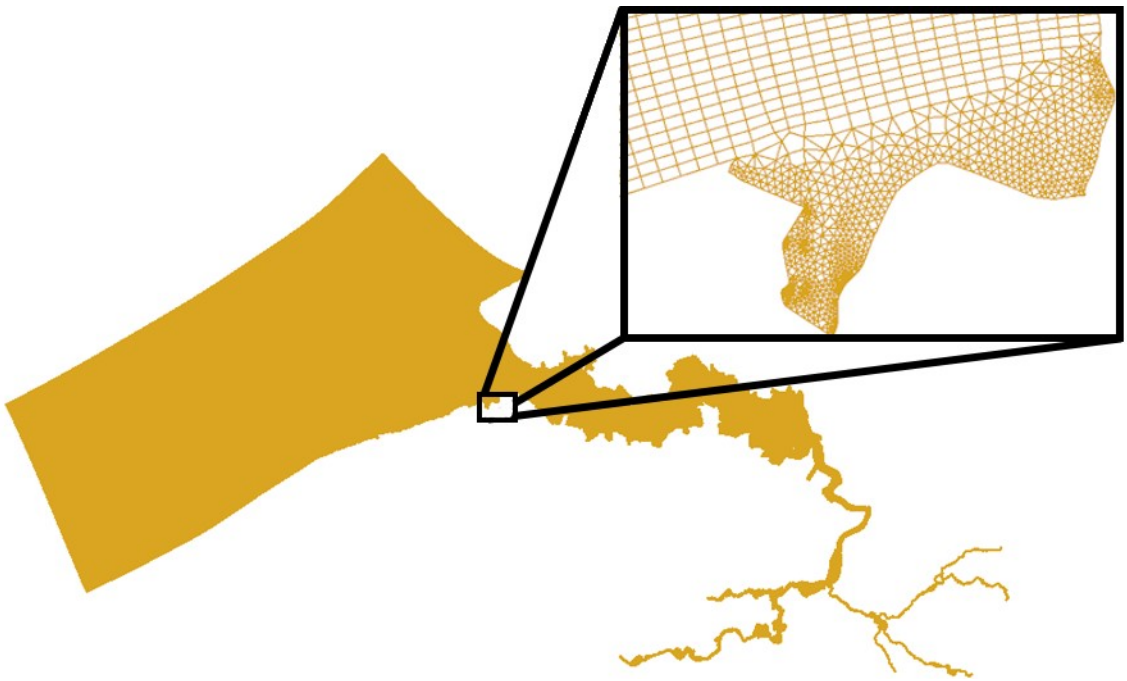

Figure 2 The model grid with a zoomed-in section of the flexible mesh of an MRS.

Cyclical Boundary Conditions

To isolate the effects of the MRS on salt intrusion, a 29-day period in June was selected as a representative period and repeated to generate 365 days of sea boundary condition input. This period was chosen as it approximately represents one spring-neap cycle under typical, calm-weather conditions. The data for this period was obtained from a hindcast of 2013-2014, as used in the original model. Further details on the selection, creation and implementation are provided in Appendix C.

At the open sea boundaries of the model domain, boundary conditions were derived from the DCSMv6-ZUNOv4 model with Kalman Filtering, as described by Zijl, et al., (2015) and Zijl, et al., (2013). This model simulates water movement for the northwestern part of the European continental shelf. In the Delft3D FM, flow and water level boundaries were applied, with flow velocities imposed perpendicular to the coast (at the North and South boundaries) and water levels prescribed parallel to the coast (at the West boundary).

Measured river discharges from 2013 were used, averaged over the entire year. Discharge rates were imposed for the Zenne, Dijle, Grote Nete, Kleine Nete, Scheldt, and Dender rivers, as well as at the sluices at Bath and Terneuzen. In Delft3D FM, all river discharges were treated as open boundaries. The discharge at every river had a psu value of 0.3.

The offshore salinity boundary conditions were set to a stable level of 32 psu. To ensure that wind did not influence the results and to avoid obscuring the model's spin-up time, wind was removed from the original model.

Initial conditions

The bed level is consistent with that used in the original model by Thiessen et al., with an average elevation selected for the MRS areas, excluding the dikes. As a result, one MRS has a bed level of

11.54 m (see Appendix A) and is too high to inundate, but this approach was maintained to ensure realistic implementation.

For salinity, the initial salinity field corresponds to the salt conditions after one year of model operation, specifically as of January 1, 2014. This provides a representation of the January salt field, although it does not exactly match the salinity conditions of January 1, 2013. Furthermore, the model is initially run with a diagnostic salinity field (excluding advection and dispersion) for six days to allow the hydrodynamics to properly spin up from a cold start. On the seventh day, the model is restarted with salinity in prognostic mode, incorporating advection and dispersion. This approach ensures that the initial salinity is combined with realistic hydrodynamic conditions.

The roughness is represented by a spatially varying Manning coefficient, ranging from 0.017 to 0.028. The specific map showing this variation can be found in Appendix A. The MRS added to the model share the same roughness coefficient as the area immediately in front of the MRS.

Managed realignment sites

The Managed Realignment Sites (MRS) selected for this study were drawn from two existing projects. These sites were chosen for their practicality, expediency, and to avoid political sensitivities about this subject. The two projects are the Sigma Plan and the “Dubble Dijken” project.

Sigma Plan

Considering climate change and rising sea levels, continued investment in the Sigma Plan is needed. This plan involves constructing higher and wider levees, establishing a network of flood control areas (FCA and FCA-CRT) along tidal rivers, and implementing localized “depoldering”. These measures are designed to protect the entire Flanders region from flooding caused by storm tides, which occur when a spring tide in the Sea Scheldt Basin coincides with a (north)westerly storm on the North Sea (Sigma Plan). The Sigma Plan has been implemented for the most part in reality; however, since the model dates to 2013, these features were not yet included. The FCA and the “depoldering” areas are used as the managed realignment sites in this paper.

Dubbele Dijken (Double Dikes)

The combination of sea-level rise and land subsidence will also necessitate the strengthening and heightening of dikes, as well as increased salinization of the land. By constructing double dikes with alternating polders, a dynamic dike zone can be created that adapts to rising sea levels without the need for additional reinforcements, thereby reducing salinization pressure. An opening would be made in the current sea dike, allowing the ebb and flood of tides to return to the land behind it, known as the alternating polder. The sea is then held back by a second dike, which could be an existing former sea dike, a sleeper dike, or a newly constructed secondary dike. This second dike can be slightly lower and more cost-effective than the current sea defense, as the first dike absorbs the energy of the water's force (WWF, 2022). This paper utilizes only the selected areas from the project, without implementing the double dike method.

The total MRS used are illustrated in Figure 1, with the "Dubbele Dijken" polygons provided by Jim van Belzen. Appendix A, Tables 1, details the dimensions of each MRS. In total, 98 MRS were added to the existing model, covering a combined area of 125.18 km^2. The MRS were incorporated into the model grid, with thin dams placed along the vicinity of the MRS. These dams were removed for the specific scenarios being simulated (e.g. all thin dams were removed for the All MRS Open scenario, see next section). The decision was made to open the thin dams along the entire length of the

boundary connected to the estuary, ensuring full connectivity between the MRS and the main channel of the estuary. Additionally, the bed level of each MRS is determined by averaging the height of the inner 90% of the MRS. This approach ensures that the dikes surrounding each MRS are excluded from the bed level calculation.

Scenarios

To assess the effect of Managed Realignment Sites (MRS) on salt intrusion and to determine if the position of these sites influences salt intrusion, a total of 5 scenarios were created. Each scenario differed based on whether specific MRS were included or excluded from the analysis. This approach allowed us to evaluate how the presence or absence of these sites impacts salt intrusion and whether their placement has an effect. The following scenarios are chosen:

1. Base scenario, no MRS are added to the model and only the existing grid was used, so all MRS are closed (scenario name: All MRS Closed).
2. All MRS open, all MRS are included in the model (scenario name: All MRS Open).
3. Enlarged Hedwige-Prosper MRS, this scenario all the MRS that are connected to the Hedwige-Prosper MRS and Hedwige-Prosper polder as well are now added to the model to symbolize a larger Hedwige-Prosper MRS to be able to see its impact clearer in the results (scenario name: Enlarged Hedwige).
4. MRS open near the mouth (Western Scheldt), this scenario includes all polders downstream of the Hedwige-Prosper polder and this scenario is chosen to see the difference between positioning closer to the mouth and further upstream (scenario name: Mouth).
5. MRS open further upstream (Sea Scheldt), this scenario includes all polders upstream of the Hedwige-Prosper polder. This scenario is chosen so it can be compared to the previous scenarios and to see what for effect the Sigma plan has on the salt intrusion length. The results can give insight of the importance of the position of the MRS. (scenario name: Upstream).

For clarity, the final three scenarios (3, 4 & 5) are illustrated in Figure 1.

Analysis of model output

The model was run for five different scenarios, with the only variation between the simulations being the inclusion or exclusion of MRS. The results that are presented are from the last 29 days of the model, to be sure that the model was fully warmed up, see Appendix C for more information. The data was collected through observation points located every 500 meters along the main channel, observation cross-sections spaced every 5000 meters, and cross-sections over each MRS, beginning at the mouth of the estuary. Figure 1 illustrates this, with the blue line indicating the main channel. The analysis will focus on the salt intrusion length, the average salinity across the entire estuary, and the tidal prism.

Results

This section presents the impact of Managed Realignment Sites (MRS) on salt intrusion at the estuary scale. Detailed analysis is provided to demonstrate how the introduction of MRS at various locations within the estuary influences salinity distribution. The results focus on comparing scenarios with and without the presence of MRS, highlighting the changes in salt intrusion length and the overall salinity gradients throughout the estuary. Lastly, the tidal prism will be analyzed and compared to the volume of the MRS.

Salt Intrusion length

Figure 3 illustrates the salinity along the SI-length for all five scenarios, based on the average of the last 29 days. It is evident that the Mouth scenario has the shortest SI-length (126 km). The Enlarged Hedwige scenario has the same result as the All MRS Closed scenario (126.8 km). The Upstream scenario shows the longest SI-length (128.5 km), extending by nearly 2.5 km compared to the shortest SI-length (scenario Mouth). The scenario All MRS open gives a SI-length of around 127.4 km.

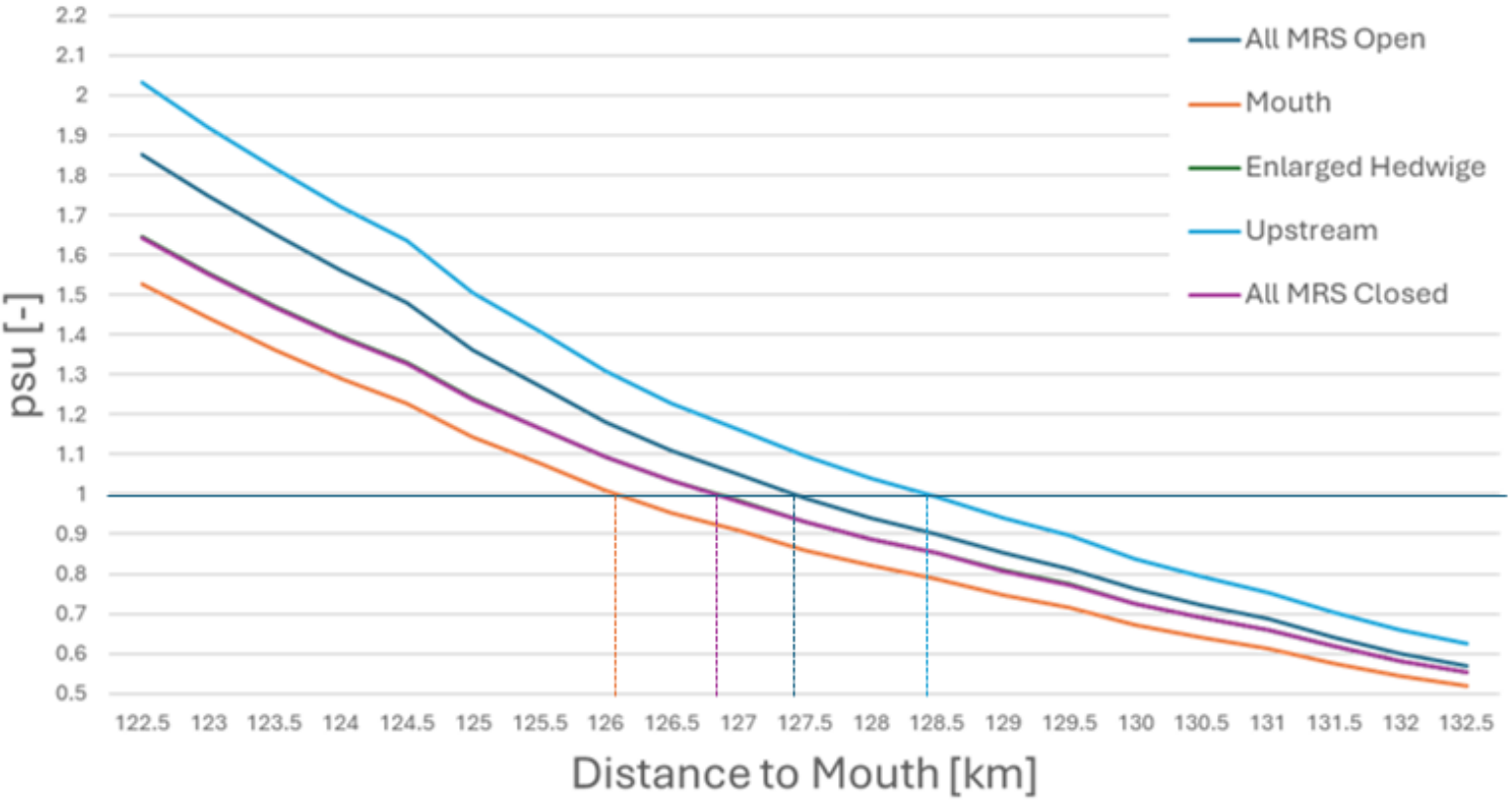

Figure 3 A zoomed-in graph of salt intrusion length for all scenarios, based on the average psu calculated from the final 29 days of simulation.

Tidal excursion

To analyze the variation in Salt Intrusion length (tidal excursion) over time, a Box and Whisker plot was created (see Figure 4). This plot shows data from the past 29 days, providing a range for the Salt Intrusion length over time. The analysis is based on 5-minute intervals, focusing on stations where the salinity (psu) is closest to 1. The results indicate minimal variation in the tidal excursion, with the range for each scenario spanning between 17 and 19 km. Additionally, the scenario with the highest

average Salt Intrusion length also displays the highest upper Whisker, while the Mouth scenario exhibits both the lowest lower Whisker and the shortest average Salt Intrusion length. The Enlarged Hedwige scenario is comparable to the All MRS Closed scenario in terms of average Salt Intrusion length, though it has a slightly smaller upper Whisker. Due to the resolution of the measurement stations (500-meter intervals), these values should be considered estimates rather than precise measurements.

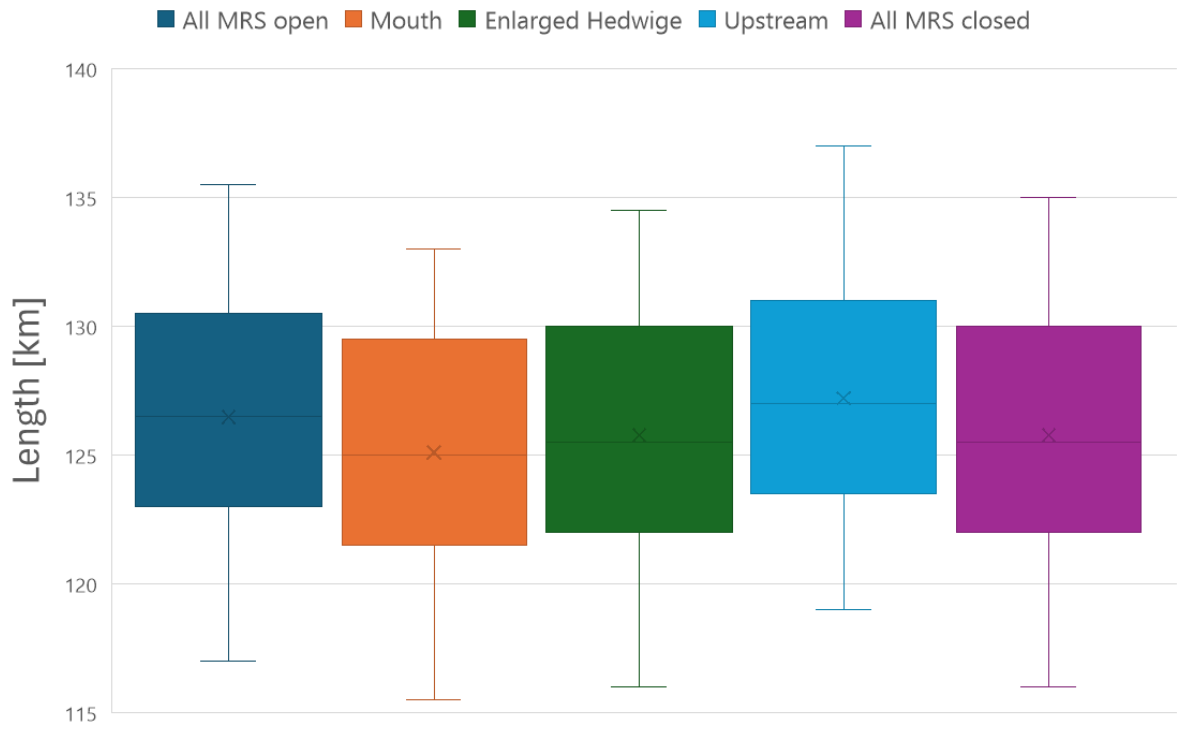

Figure 4 Box and Whisker plot showing all scenarios, using data collected every 5 minutes over the final 29 days without averaging. The cross resembles the average, the line the median and the points the outliers.

Average salinity

Figures 3 and 4 present only the SI-length, offering a narrow perspective that reflects just the average length at the location where the salinity (psu) equals 1. Additional salinity variations are illustrated in Figure 5, which examines the entire length of the estuary. A distinct S-curve pattern emerges in the Mouth scenario, where salinity increases by 0.4 psu just before the Hedwige MRS (indicated by the red line) compared to the All MRS Closed scenario and decreases by 0.17 psu further upstream. In the Upstream scenario, the opposite trend is observed, with a more pronounced peak, a 0.6 psu increase in salinity, occurring after the Hedwige MRS. The Enlarged Hedwige scenario has only a minor effect on salinity levels in the vicinity of the MRS, with changes ranging between -0.03 and 0.08 psu. The scenario in which all MRS are opened shows characteristics resembling a combination of the other three scenarios, blending elements of the Mouth, Upstream, and Enlarged Hedwige scenarios. Overall, there is no significant absolute difference in salinity (psu) across the scenarios, with the psu values never changing by more than 0.6. Figure 5 displays the relative psu values compared to the average psu of the All MRS Closed scenario, allowing for a clearer assessment of the scenarios' impacts. Notably, a 24% increase in salinity is observed in the upstream region (beyond Hedwige MRS) under the Upstream scenario, while the All MRS Open scenario shows a maximum increase of 14%, and the Mouth scenario sees a decrease of 8%.

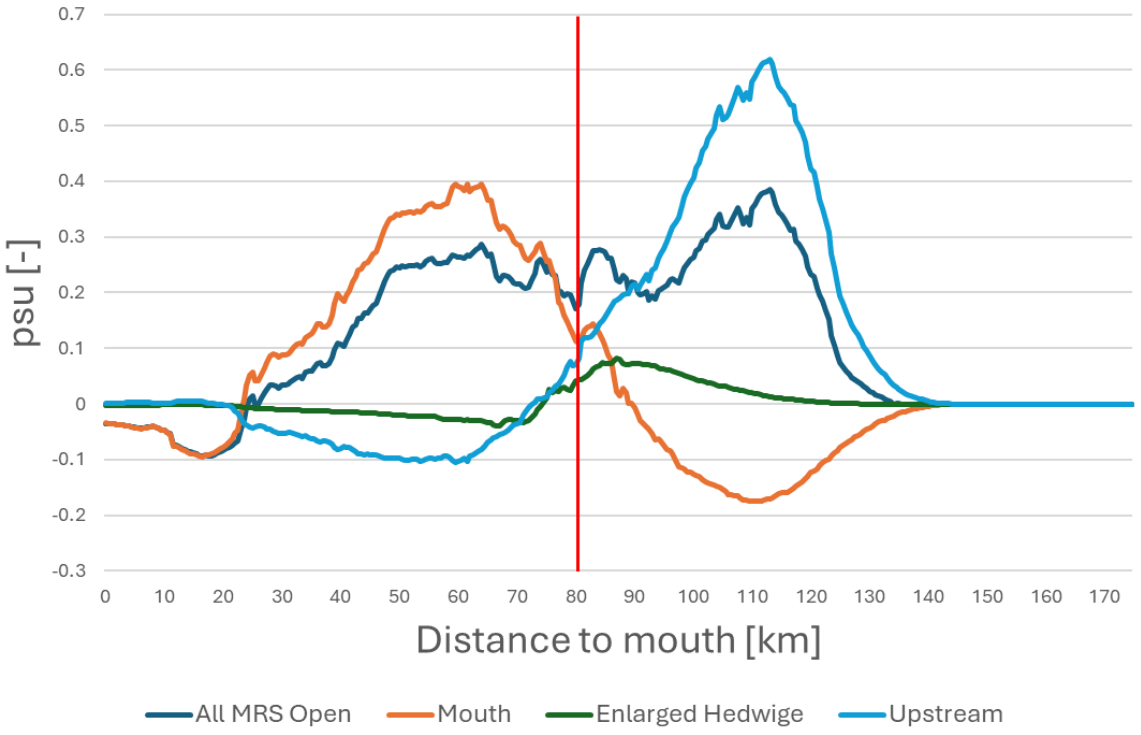

Figure 5 Difference psu value plot compared to the All MRS Closed scenario per tide of the last 29 days of the simulation, in red showing the location of the Hedwige MRS.

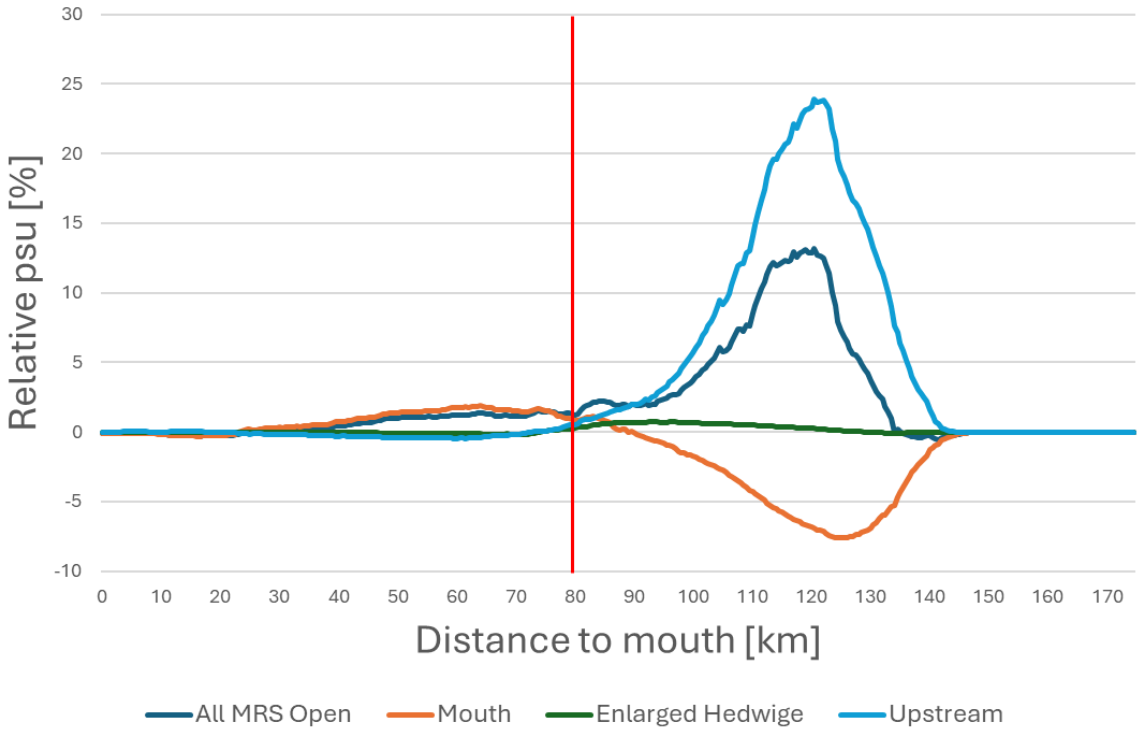

Figure 6 Relative effect of the psu average difference between the All MRS Closed scenario, in red showing the location of the Hedwige MRS.

Tidal Prism

To identify the processes influencing the outcomes described above, we compare the tidal prism differences across the entire estuary relative to the All MRS Closed scenario. Figure 7 presents the relative differences in tidal prism between the All MRS Closed scenario and the other four scenarios. A clear pattern emerges, closely aligning with the trends observed in the average psu graphs above. In the Mouth scenario, salinity increases by up to 4% before the Hedwige MRS and decreases by 2.5% afterward. In contrast, the Upstream scenario shows the opposite trend, with a smaller 1% increase before the Hedwige MRS and a larger 7% peak after it. The All MRS Open scenario once again displays a combination of features from the other scenarios, reflecting elements of both the Mouth and Upstream patterns. Far upstream of the estuary, there is a significant decrease, which can be attributed to the locks included in the model; however, this aspect is not the focus of the current research. Given the well-mixed nature of the Scheldt estuary, salt intrusion is primarily governed by the tidal oscillatory (depth-averaged) salt flux and the net flow (mainly river discharge). A significant increase in the tidal prism leads to a greater tidal oscillatory salt flux, allowing more saline water to enter the system. In the Upstream scenario, the larger tidal prism at 110 km likely amplifies the tidal oscillatory salt flux, pushing more saline water further upstream and increasing salt intrusion. However, it is important to note that, by definition, tidal prism alone does not alter the tidal oscillatory salt flux. Such changes only occur when the tidal flow is asymmetrical, which is assumed in these simulations. This process is one of the key factors explaining the observed increase in salt intrusion length under the Upstream scenario, as shown in Figure 3. Conversely, in the Mouth scenario, the smaller tidal prism observed after the Hedwige polder suggests a reduced tidal oscillatory salt flux, which limits the amount of saline water entering the system and results in a factor that shortens the salt intrusion length.

Overall, it is evident that the Upstream scenario exerts the most significant influence on both psu and tidal prism, even though the MRS areas involved are relatively small (as detailed in Appendix A). To further investigate this, Figure 8 has been created, illustrating the volume of water collected during a single tide, averaged over the last 29 days of a MRS, divided by the local tidal prism within the channel near the specific MRS. The MRS ID corresponds to a specific MRS, as detailed in Appendix A. Additionally, MRS ID 1 is the closest to the mouth of the estuary, with higher ID numbers indicating locations further upstream. This figure demonstrates the impact that an MRS can have on local tidal prism based on its volume. The highest ratios are observed upstream of the Hedwige MRS, highlighted in red. These results align with the findings above (relative psu and relative tidal prism), showing that the most significant differences occurred upstream due to this impact.

Figure 7 Relative effect of the tidal prism, in red the location of the Hedwige MRS.

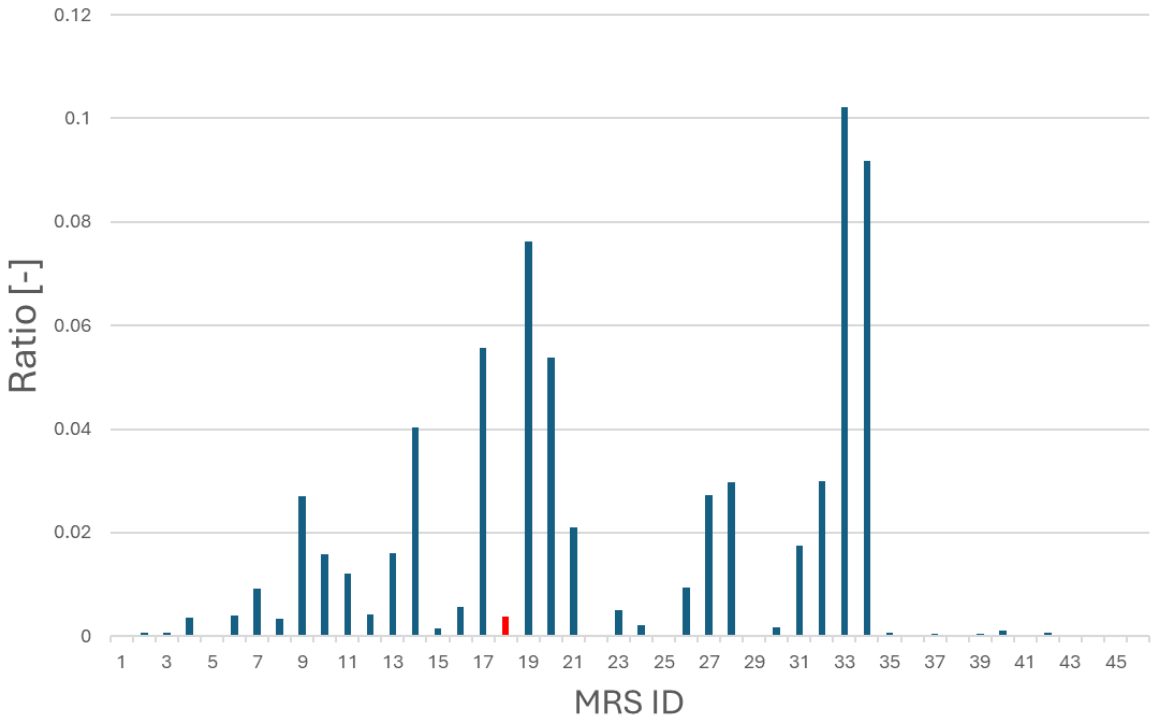

Figure 8 Ratio of the volume of the MRS divided by the local tidal prism near to that specific MRS. Each bar represents a MRS and the red bar is the Hedwige MRS.

Comparison with existing literature

Hendrickx et al. (2014) states: " For both the salt wedge and partially mixed estuary classes, an increased areal ratio reduces the salt intrusion length, while the opposite is true for the well-mixed estuary. In case of the well-mixed estuary, increasing the intertidal area can more than double the salt intrusion length compared to the reference case (i.e., without intertidal area)." In this study, the entire estuary boundary is designated as MRS and fully connected to the sea, with no barriers separating the MRS from the sea. As the size of this intertidal area increases, so does the SI-length. The scenario that most closely resembles the idealized estuary schematization used in this study is the All MRS open scenario. In both this study and the research by Hendrickx et al., an increase in SI-length was observed. This study found no instances of salt intrusion doubling; the maximum observed increase was less than 1 km for an SI-length of approximately 127 km. It is important to note that the additional MRS area in this study is much smaller compared to the Hendrickx et al. study, where the SI-length doubled. In that case, the areal ratio was around 0.28, while in this study, it is around 0.056. Additionally, the connectivity to the sea differs significantly, as there is no direct open connection between the MRS and the sea in this study, so all salt transport into the estuary comes through the channel. Moreover, the results in this paper indicate that the impact of added intertidal area depends heavily on its location. Specifically, when additional area is added near the mouth of the estuary, the SI-length can even be reduced.

In the study by Stark et al. (2017), a comparable methodology is employed to investigate the impact of MRS on hydrodynamics. One of the processes examined was the relative tidal prism, as illustrated in Figure 9. Comparing this figure with the results of the relative local tidal prism in this paper (Figure 7), it shows similar trends. First, looking at the MRS closer to the mouth (KM-12 and KM-28) and the Mouth scenario in this paper. Both show in effect of increasing the relative tidal prism near the mouth and both show a small gentle flat peak. Secondly, looking at the more upstream MRS (KM-66 and KM-97) and the scenario Upstream both a steeper peak more upstream and near the MRS location. Furthermore, Stark et al. (2017) observed: "The effect of additional intertidal storage areas on the tidal prism varies along the estuary. Upstream of these storage areas, there is a reduction in tidal prism, which is more pronounced the further upstream the area is located" (see Figure 9). This pattern is also evident in Figure 7 of this paper, though it features smaller peaks of relative tidal prism rather than a flat line. This difference arises because Stark's study focused on four individual intertidal areas, while the current paper examines the simultaneous impact of multiple MRS, leading to additional peaks due to the influence of the smaller MRS. The absolute values can not be compared to the difference between the volume of the MRS that were attached in both studies. The largest volume of the MRS in this paper is 18 Mm^3 whereas Stark et al. examined MRS with a minimum volume 47 Mm^3.

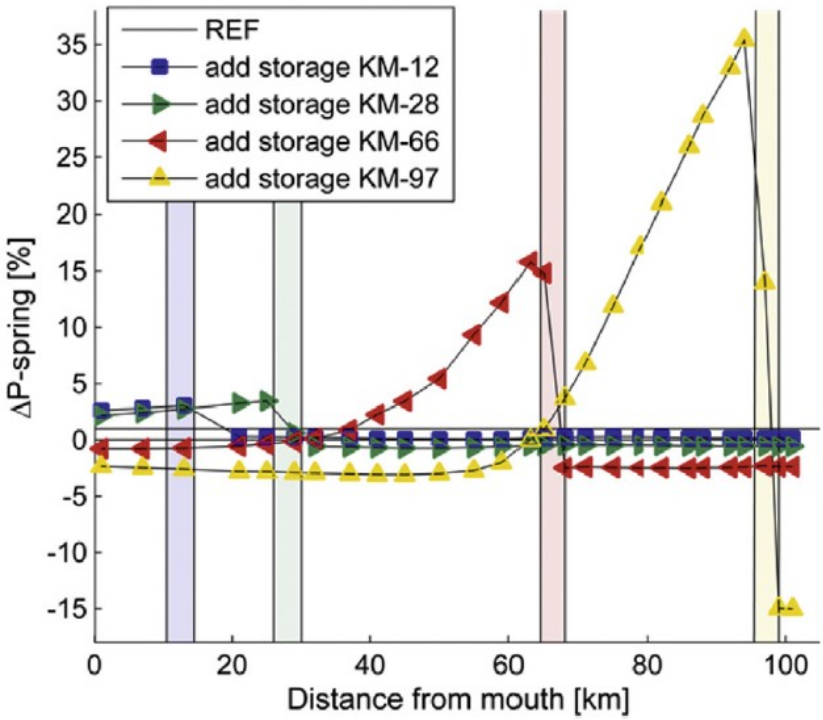

Figure 9 Modelled percentage change in tidal prism for the scenarios with added MRS (KM-12 (blue), KM-28 (green), KM-66 (red) and KM-97 (yellow) compared to the reference scenario (zero line)). [source: Stark et al. (2017)]

Discussion

In this paper a numerical shallow water model (Delft3D FM) is used to be able to give an insight of the impact of MRS on the salt intrusion in the Scheldt estuary. The main finding revealed that the average salt intrusion length decreased when MRS were implemented near the estuary's mouth and increased when MRS were added further upstream. Additionally, at the estuary scale, a S-curve pattern in average salinity was observed: when MRS were added near the mouth, salinity initially increased near the mouth and decreased further upstream, while the opposite effect occurred when MRS were implemented upstream. A similar pattern was observed in the relative tidal prism, which helps explain the results of the average salinity. Furthermore, these results were compared to earlier studies, revealing clear and consistent patterns. For example, the increase in salt intrusion length when all MRS were open was consistent with findings from an idealized schematization of the estuary modelling study. Similarly, the trends in relative tidal prism were comparable to those observed in a study that examined the impact of adding MRS on tidal prism. While the model is not perfect, the results offer a good representation of real-world conditions and provide a consistent initial understanding of the impact of MRS. However, it is important to acknowledge that further improvements and additional topics need to be addressed.

The model used in this paper assumes static estuarine morphology, which limits its ability to accurately predict the long-term effects of MRS on salt intrusion. Given that estuarine morphology is dynamic and evolves over time due to interactions with hydrodynamic and ecological processes, this static assumption may affect the predictions. However, given that the impact of a large MRS is already relatively small (maximum 2km difference with All MRS closed), the variations in bed level will have a minimal effect on the overall outcomes related to SI-length.

Furthermore, a 2D version of Delft3D FM is used to calculate salinity, providing an overview of the SI-length and insights into general dynamics. However, this 2D approach lacks the ability to fully capture the complexity of salinity distribution and movement. A significant limitation is its inability to model gravitational circulation—a crucial 3D process where denser, saltier water moves landward along the bottom while lighter, fresher water flows seaward at the surface. The absence of vertical stratification and mixing representation can lead to inaccuracies in predicting salinity gradients. Additionally, the 2D model does not adequately simulate vertical mixing caused by wind-driven turbulence or other 3D processes, such as lateral circulation influenced by Coriolis forces. Consequently, 2D calculations may oversimplify or misses the mentioned above key aspects of estuarine salinity dynamics. Nonetheless, since the Scheldt estuary is well-mixed, with relatively uniform saline water columns, many of these limitations are less problematic in this context. Furthermore, the computational demands of conducting detailed research with this model are a key reason for not using a 3D model. In this study, even with a supercomputer, it took five full days to simulate one year. As shown in Appendix C, Figure 18, the model requires a spin-up time of approximately seven months. Therefore, the full one-year simulation is essential, and using a 3D model would significantly multiply the computational time required.

Moreover, the existing model used in this study contains salinity errors measured over 4 stations (in the margin of 0,42-0.88 R^2) (Vroom et al., 2015), meaning the absolute values of the results cannot be directly compared to real estuary conditions. As previously mentioned, this study builds upon existing research, and the results demonstrate consistent and clear patterns that align with earlier findings. This consistency indicates a level of robustness in the research, which could be valuable for informing decision-making.

Another factor that influenced the salt intrusion length absolute value was the resolution of the measuring stations, which were spaced 500 meters apart. Due to the spacing, the actual salt intrusion length could vary within a range of 251 to 749 meters. This lack of precision means that the reported intrusion length may not fully capture the finer-scale variations in salinity distribution, potentially leading to an underestimation or overestimation of the true salt intrusion length. To address this issue, a denser array of measurement points near the estimated salt intrusion length could be implemented. For instance, in this study, the resolution could be refined to every 50 meters between 120 and 130 km.

The observed impact on salt intrusion length is approximately 2 km, with an average increase of 0.6 psu across the estuary. While these changes are relatively small compared to existing values, Hendrickx et al. (2024) indicate that the salt intrusion length could potentially double when the areal (area of MRS/ channel area) is 0.28. This suggests that areal configuration can significantly influence salt intrusion length. However, it is important to note that this study found out that there is a balance between MRS located near the mouth and those positioned upstream. Strategically positioning the areal could therefore be more beneficial for enhancing the impact on salt intrusion length.

The MRS used in the model are replicated from other existing projects without customization of the location. Additionally, the areas in the Netherlands included in the model are still partially inhabited, with no current plans for inundation or restoration to the estuary, making it unlikely that this scenario will occur. As a result, the findings of this paper should be viewed more as illustrative examples rather than predictions of actual future conditions. Furthermore, the bed levels of the MRS are averaged across the entire area, a simplification that maintains the storage volume of each MRS, but that would not be implemented as such in the field. In addition, nothing can be said about the influence of bed level of these MRS towards the salt intrusion.

Conclusion

An updated version of the Delft3D FM NeVla model was modified to include MRS in the grid and was subsequently used to assess the impact of MRS on salt intrusion in a well-mixed estuary. The model results indicated that, on average, the salt intrusion length increased in scenarios where multiple MRS were opened upstream (1700 m) or where MRS were opened both upstream and near the mouth (600 m). Conversely, the salt intrusion length decreased only in the scenario where MRS near the mouth were opened (600 m). No significant changes in salt intrusion length were observed when a single large MRS was opened in the middle of the estuary. Analysis of the average salinity across the estuary for both the Mouth and Upstream scenarios revealed an S-curve pattern, which was also observed in the tidal prism data. Additionally, the maximum percentage increase in salinity was 24%, while the maximum decrease was 8%. These findings are consistent with existing studies.

Recommendations

For future research, it is recommended to incorporate morphological changes into the model to create a more realistic representation that includes the development and dynamics of intertidal creeks. Such an approach would allow for a deeper understanding of how these areas evolve over time. A prime example is the Drowned Land of Saeftinghe, an intertidal zone preserved for nature, which has gradually transformed into one of the highest elevated areas in the region. Such elevation gain can significantly affect the volume of the MRS, potentially reducing it over time. Understanding how this reduction impacts salt intrusion length is crucial for assessing long-term estuarine dynamics.

Additionally, this study is focused solely on the Scheldt estuary, which is classified as a well-mixed estuary. In such estuaries, 2D modeling has a limited impact on predicting salt intrusion length due to the relatively uniform over depth distribution of salinity. However, it would be valuable to extend this type of analysis to estuaries with different classifications, such as partially mixed or stratified estuaries. In these environments, vertical variations in salinity and the influence of gravitational circulation play a much more significant role in salt intrusion. Therefore, a 2D model would likely be insufficient for capturing these complexities. A 3D model would be recommended in these cases to accurately represent the effects of gravitational circulation, stratification, and other vertical processes on salt intrusion dynamics. Conducting such studies across various estuarine types would provide a more comprehensive understanding of the factors influencing salt. Additionally, improving the resolution near the salt intrusion length would be beneficial, especially given the subtle effects of MRS, to ensure that all relevant information is captured.

Moreover, this study uses an 29 days cyclical form of forcing to ensure the complete spin-up of the model. While this approach is effective for stabilizing the model, it does not account for the impact of extreme weather events such as storms or droughts. These events can significantly alter estuarine dynamics, introducing conditions like reduced river discharge or elevated sea levels, all of which are not represented in the current model.

For example, drought conditions could be simulated by reducing the discharge rates in the model, mimicking the lower freshwater input typical of such periods. Including these scenarios in future studies would provide a more comprehensive understanding of the estuary's behavior under varying climatic conditions and help to assess the resilience of estuarine systems to extreme events. This would enhance the model's predictive accuracy and make it more applicable to real-world situations, where such events can have significant impacts on salt intrusion and other estuarine processes.

The tidal prism is identified as a factor influencing salt intrusion length; however, it affects the tidal oscillatory salt flux primarily when the tide is asymmetrical. Due to time constraints in this study, further research on tidal asymmetry and its changes resulting from MRS was not conducted. Exploring these aspects could provide greater insight into the mechanisms behind changes in salt intrusion length and offer better estimations for similar processes in other estuaries.

Lastly, the influence of bed level height within the MRS plays a significant role in determining estuarine dynamics, yet this factor was not thoroughly investigated in this study. The chosen MRS configurations were based on existing projects, leading to the use of average bed levels specific to those sites. As a result, the study did not explore how variations in bed level height might affect outcomes. Although the ratio of added volume to local tidal prism was investigated.

It would be valuable to conduct further research by designing scenarios with MRS of varying bed heights, comparing them to scenarios where MRS have uniform heights. By keeping the positions of the MRS relatively constant between scenarios, it would be possible to isolate and analyze the impact of bed level height on estuarine processes, such as salt intrusion. This approach would offer insights into how variations in bed level affect the performance and behavior of MRS under real-world conditions. Although the ratio of added volume to the local tidal prism was examined in this paper. The outcomes could then be able to compare it to the study of Hendrickx et al. (2024).

By understanding the intricate dynamics of salt intrusion and the influence of factors like bed level height, morphological changes, and extreme weather events, policymakers could craft more effective strategies to manage estuarine environments. This would ensure that salinity levels are optimized to support biodiversity while also meeting the needs of industries and communities that rely on these water systems.

References

Bennet, W. G., Veelen, T. J., Fairchild, T. P., Griffin, J. N., & Karunarathna, H. (2020). Computational Modelling of the Impacts of Saltmarsh Management Interventions on Hydrodynamics of a Small Macro-Tidal Estuary. *JMSE*.

Braeckel, A. V., Vandervoorde, B., & Bergh, E. V. (2008). TIDAL MARSH MODELLING IN THE SCHELDT ESTUARY: DETERMINE RESTORATION POTENTIALS FOR MANAGED. *6th European Conference on Ecological Restoration.* Ghent.

Deltares . (2024). *D-flow flexible Mesh User Manual .* Delft: Deltares.

Environmental Protection Agency. (2023). Climate Adaption and Estuaries. USA.

Fossati, M., & Piedra-Cueva, I. (2013). A 3D hydrodynamic numerical model of the Río de la Plata and Montevideo's coastal zone. *Applied Mathematical Modelling*.

French, P. W. (2006). The developing story of a comparatively new approach to soft engineering . *Estuary Coastal Shelf Science*, 409-423.

Geyer, W. R., & MacCready, P. (2014). The Estuarine Circulation. *The Annual Review of Fluid Mechanics* , 175-197.

Geyer, W. R., Raltson, D. K., & Chen, J. L. (2020). Mechanisms of exchange flow in an estuary with a narrow, deep channel and wide, shallow shoals. *Journal of Geophysical Research*.

Guerra-Chanis, G. E., Laurel-Castillo, J. A., Schettini, C. A., Kakoulaki, G., Souza, A. J., & Valle-Levinson, A. (2022). Saltwater intrusion in estuaries with different dynamic depths. *Regional Studies in Marine Science, 51*.

Hendrickx, G. G., & Pearson, S. G. (2024). On the effects of intertidal area on estuarine salt intrusion. *JGR Oceans*.

Hendrickx, G., Kranenburg, W., Antolinez, J., Huismans, Y., Aarninkhof, S., & Herman, P. (2023). Sensitivity of salt intrusion to estuary-scale changes: A systematic modelling study towards nature-based mitigation measures. *Estuarine, Coastal and Shelf Science, 295*.

Interreg North Sea Region IMMERSE. (n.d.). *The SCheldt Estuary.* https://northsearegion.eu/immerse/project-estuaries/the-scheldt-estuary.

Kim, K. B., Kwon, H., & Han, D. (2018). Exploration of warm-up period in conceptual hydrological modelling. *Journal of Hydrology*.

Lyu, H., & Zhu, J. (2019). Impacts of tidal flat reclamation on saltwater intrusion and freshwater resources in the changjiang estuary. *Journal of Coastal Research*, 13209-13216.

Meire, P., Ysebaert, T., Damme, S. V., Bergh, E. V., Maris, T., & Herman, P. (2005). The Scheldt estuary: a description of a changing ecosystem. . *Hydrobiologia, 540*, 1-11.

Mohammed, R., & Scholz, M. (2018). Critical review of salinity intrusion in rivers and estuaries . *Journal of Water & Climate Change, 9*(1), 1-16.

Mondal, P., Walter, M., Miller, J., Epanchin-Niell, R., Yawatkar, V., Nguyen, E., & Tully, K. L. (2023). The spread and cost of saltwater intrusion in the US Mid-Atlantic. *Nature Sustainability*, 1352-1362.

Nesvarova, M. (2024). UT scientists test living dikes in 'the first experiment of its kind'. In *Utoday.*

Pontee, N. (2015). Impact of managed realingment design on estuarine water levels. *Maritime Engineering* , 48-61.

Pritchard, D. W. (1967). What is an estuary: physical viewpoint. *American Association for the Advancement of Science*, 149-176.

Raltson, D. K., & Geyer, W. R. (2019). Response to channel deepening of the salinity intrusion, estuarine circulation, and stratification in an urbanized estuary. *Journal of Geophysical Research: Oceans*, 4784-4802.

Savenije, H. H. (2005). *Salinity and Tides in Alluvial Estuaries.*

Siemes, R., Duong, T., Borsje, B., & S.Hulscher. (2023). Estuarine salt intrusion affected by channel depth,. In *Book of Abstracts* (Vol. "not yet published").

Sigma Plan. (n.d.). *Protecting Flanders, today and tomorrow.* https://www.sigmaplan.be/en/themes/security.

Smolders, S., Kapitein, S., Ozkier, S., & Stark, J. (2023). *Zoutgradient in het Schelde-estuarium: Deelrapport 1 - literatuuronderzoek en data-analyze.* Antwerpen: Waterbouwkundig Laboratorium.

Stark, J., Smolders, S., Meire, P., & Temmerman, S. (2017). Impact of intertidal area characteristics on estuarine tidal. *Estuarine, Coastal and Shelf Science*, 138-155.

Tiessen, M., Vroom, J., & Werf, J. v. (2016). *Ontwikkeling van het Delft3D FM NeVla model voor het Schelde estuarium .* Deltares.

Vanlede, J., Delecluyse, K., Primo, B., Leyssen, G., Plancke, Y., Vewaest, T., & Mostaert, F. (2015). *Verbetering randvoorwaardenmodel: Subreport 7 - Calibration of NEVLA 3D. Version 4.0. WL Rapporten.* Antwerp: Flanders Hydraulics Research & IMDC.

Vriend, H. J., Wang, Z. B., Ysebaert, T., Herman, P. M., & Ding, P. (2011). Eco-Morphological Problems in the Yangtze Estuary and the Western Scheldt. *Eco-Healthy Estuarine Wetlands*.

Vroom, J., Vet, L. d., & Werf, J. v. (2015). *Validatie waterbeweging Delft3D-NeVla model Westerscheldemonding.* Deltares.

Vroom, J., Vet, P. L., & Werf, J. J. (2015). *Validatie waterbeweging Delft3D NeVla model Westerscheldemonding.* Delft: Deltares.

Wang, Z. B., Vandenbruwaene, W., Taal, M., & Winterwerp, H. (2019). Amplification and deformation of tidal wave in the Upper Scheldt Estuary. *Ocean Dynamcis*, 829-839.

Weiqiu. (2024). The effectiveness of nature-based solutions in mitigating salt intrusion in estuaries: review. *not published*.

Weisscher, S., Baar, A., Belzen, J. v., Bouma, T., & Kleinhans, M. (2022). Transitional polders along estuaries: Driving land-level rise and reducing. *Nature-Based Solutions*.

WWF. (2022). *Dubbele dijken als robuuste waterkerende landschappen.*

Zhou, J., Stacey, M. T., Bouma, T. J., Bricker, J., Townend, I., Wen, J., . . . Cai, H. (2021). Tidal-flat reclamation aggravates potential risk from storm impacts. *Coastal Engineering*.

Zijl, F., Sumihar, J., & Verlaan, M. (2015). Application of data assimilation for improved operational water-level forecasting on the Northwest European Shelf and North Sea. *Ocean Dynamics*.

Zijl, F., Verlaan, M., & Gerritsen, H. (2013). Improved water-level forecasting for the Northwest European Shelf and North Sea through direct modelling of tide, surge and interaction. *Ocean Dynamics*.

Appendix

A. Information of the MRS

Due to the politically sensitive nature of the topic, no new managed realignment sites were proposed. The MRS used in this study are based on the "Dubbele Dijken" and Sigma Plan projects. All MRS (98) are listed in the graphs and tables below, with the Mouth scenario shown in red, the Enlarged Hedwige scenario in green, and the Upstream scenario in yellow. Each number represents one or more MRS (MRS located adjacent to each other combine to form a larger continuous area) and is associated with an averaged bed level height, excluding the dikes within these sites. This is calculated by averaging the inner 90% of the MRS area, the specific values provided in Table 1. Additionally, the table includes the volume of each MRS, determined by averaging the total water movement in and out of the MRS during a tidal cycle over the past 29 days. A similar approach was applied to calculate the local tidal prism, measuring the water volume crossing a closed cross-section observation line (spaced every 5000 m from the mouth) per tide, averaged over the same period. Figure 10 below shows the location of the MRS

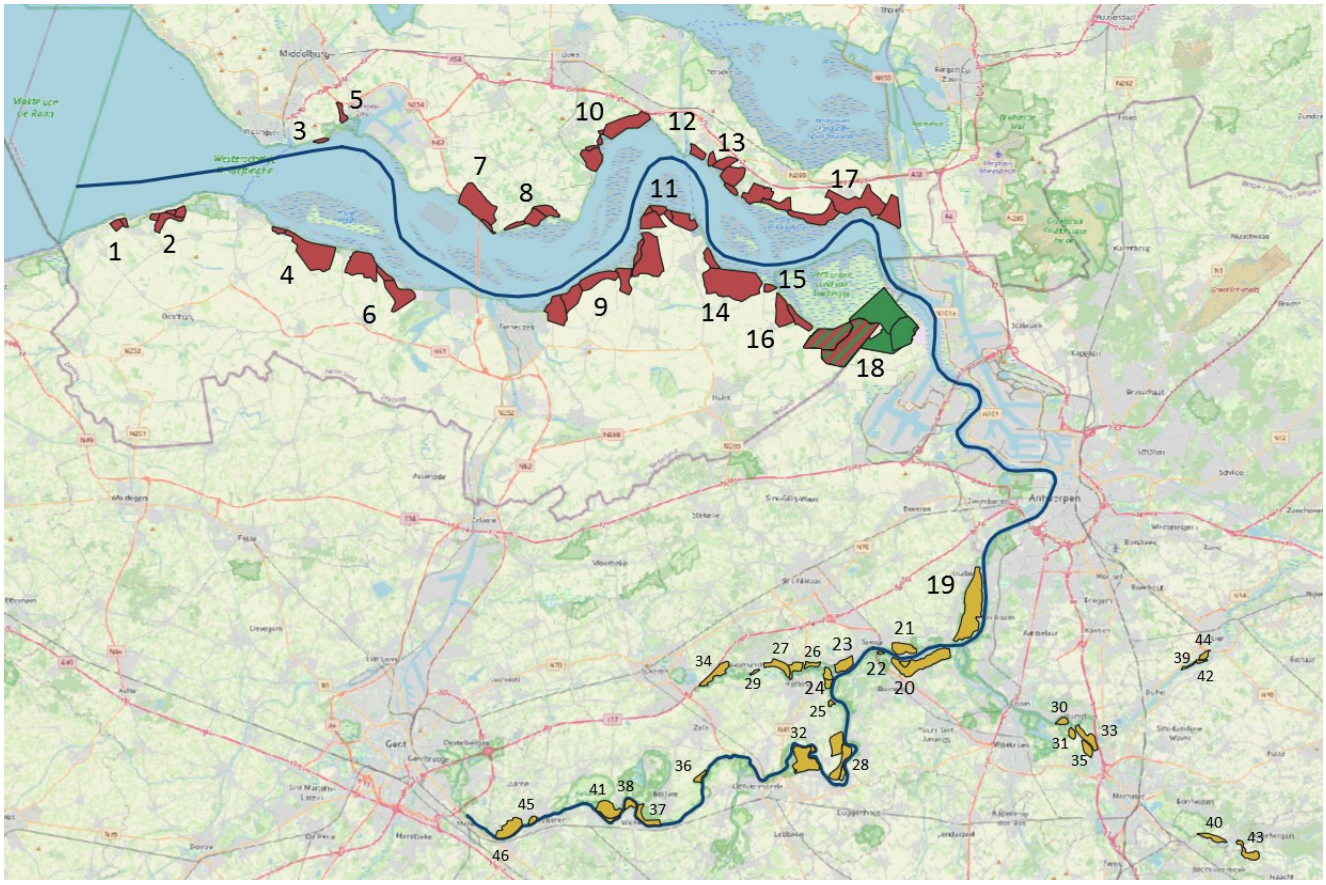

Figure 10 Map of the Scheldt Estuary highlighting key areas: the Mouth (red), Enlarged Hedwige (green), and Upstream scenarios (yellow). The blue line represents the main channel, along which data is collected every 500 meters. This line is also used to mark the observation cross sections at 5000-meter intervals.

ID	Volume [Mm3]	Area [ha]	Local tidal prism [Mm3]	Ratio volume/total water * 100 [%]	Height [m + NAP]	Distance from mouth [km]
1	0.120849	71.0068	1352.659808	0.008934	1.62	2.5
2	0.860243	209.9395	1352.659808	0.063596	1.48	7
3	0.69287	23.1124	1165.501668	0.059448	-0.26	18

4	3.920849	523.9086	1073.653797	0.365187	1.86	19
5	0.204935	50.797	1073.653797	0.019088	1.63	19.5
6	3.911704	625.9933	981.629932	0.398491	1.65	28.5
7	8.244258	455.0201	903.301034	0.912681	0.16	32
8	2.51222	247.0779	736.651612	0.341032	1.2	40
9	18.018452	814.6181	665.844559	2.706105	1.2	44
10	9.267233	532.2718	588.313908	1.575219	0.97	52.5
11	5.99613	396.964	498.526929	1.20277	1.09	54
12	2.063977	70.0774	498.526929	0.414015	0.16	55.5
13	6.933911	353.0428	434.883309	1.59443	0.55	57.5
14	14.566334	822.4134	361.551626	4.028839	0.69	63.5
15	0.51897	36.9291	361.551626	0.14354	1.37	66.5
16	1.662191	306.9565	291.048566	0.571104	1.28	71
17	16.21736	1211.2756	291.048566	5.572046	1.29	71.5
18	0.898114	1374.7324	234.137423	0.383584	1.61	79
19	5.333843	543.6874	70.038494	7.615588	1.73	115
20	1.926344	22.9962	35.78478	5.383138	1.74	122.5
21	0.749772	115.5002	35.78478	2.095226	2.18	122.5
22	0.004638	7.7314	30.78478	0.015066	11.54	124.5
23	0.152185	96.4574	30.78478	0.494351	2.76	128
24	0.049378	73.1155	23.282069	0.212086	3.03	129
25	0.000026	12.9638	23.282069	0.000112	1.3	130
26	0.004646	32.7845	0.495912	0.93686	4.94	132
27	0.013494	64.2393	0.495912	2.721047	5.13	135
28	0.525709	26.7041	17.726715	2.965631	2.51	136
29	0	10.5471	0.13997	0	5.5	138
30	0.012377	33.6876	7.555262	0.16382	4.45	139.5
31	0.132238	29.4385	7.555262	1.750277	2.4	142.5
32	0.43159	11.6915	14.380337	3.001251	2.48	143
33	0.772068	100.2293	7.555262	10.21894	1.93	144
34	0.001	115.3023	0.010906	9.169265	4.15	145
35	0.005077	54.4802	7.555262	0.067198	3.68	145
36	0.002211	33.1094	7.962397	0.027768	4.3	154
37	0.002273	84.7365	6.252958	0.036351	4.03	161
38	0.001058	41.376	4.634905	0.022827	4.23	163.5
39	0.000584	13.6196	1.389116	0.042041	4.78	164.5
40	0.000675	58.0915	0.62723	0.107616	6.5	165
41	0	24.8258	4.634905	0	4.18	166
42	0.000962	13.1095	1.389116	0.069253	4.78	166.5
43	0.000061	82.6197	0.62723	0.009725	7.58	167
44	0.000004	28.4942	1.389116	0.000288	4.19	167
45	0	23.0571	3.259568	0	4.27	172
46	0	159.6005	2.105343	0	5.2	174

Table 1 Information MRS

The roughness map is shown in Figure 11.

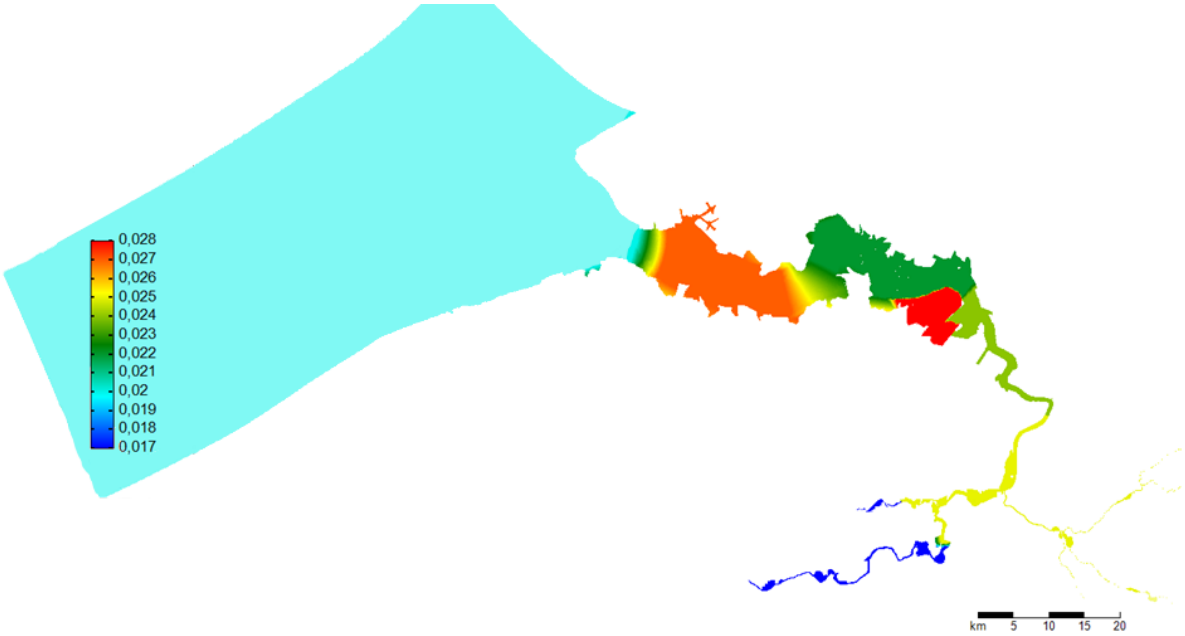

The water level remains unchanged, and the MRS areas start without an initial water level.

Figure 11 Manning coefficient map in the model, with darker shades of red indicating higher roughness.

B. Grid development

The original model grid developed by Flanders Hydraulics was enhanced by incorporating the chosen MRS using the flexible mesh option, allowing for the implementation of complex geometries to the existing grid. The polygons used in this process, which were provided by two collaborating institutes, underwent minor adjustments to enhance the accuracy of their shapes and positions, making them highly representative of real-world conditions.

Initially, the polygons were imported into the RGFGRID software. The vertices defining each polygon were either smoothed or extend with additional points to ensure that the polygon resolution aligned closely with the existing grid structure. This step required careful balancing to preserve the physical integrity of the curves while avoiding the creation of excessively small grid cells (see Figure 12 for an illustration). Subsequently, the "grow grid from polygon" function within RGFGRID was used to generate the Flexible Mesh of the new MRS.

The newly created MRS grid was then integrated with the existing model grid. For the model to function effectively, the orthogonality of the grid needed to be below 0.5, with an optimal target around 0.05. To meet these requirements, certain outer points of the polygons were adjusted, leading to minor modifications in the MRS grid. The maximum orthogonality value achieved by the newly generated grid, with all MRS incorporated, was 0.188, with overall values presented in Figure 15. The entire process of integrating a single MRS into the existing grid is detailed in Figure 13.

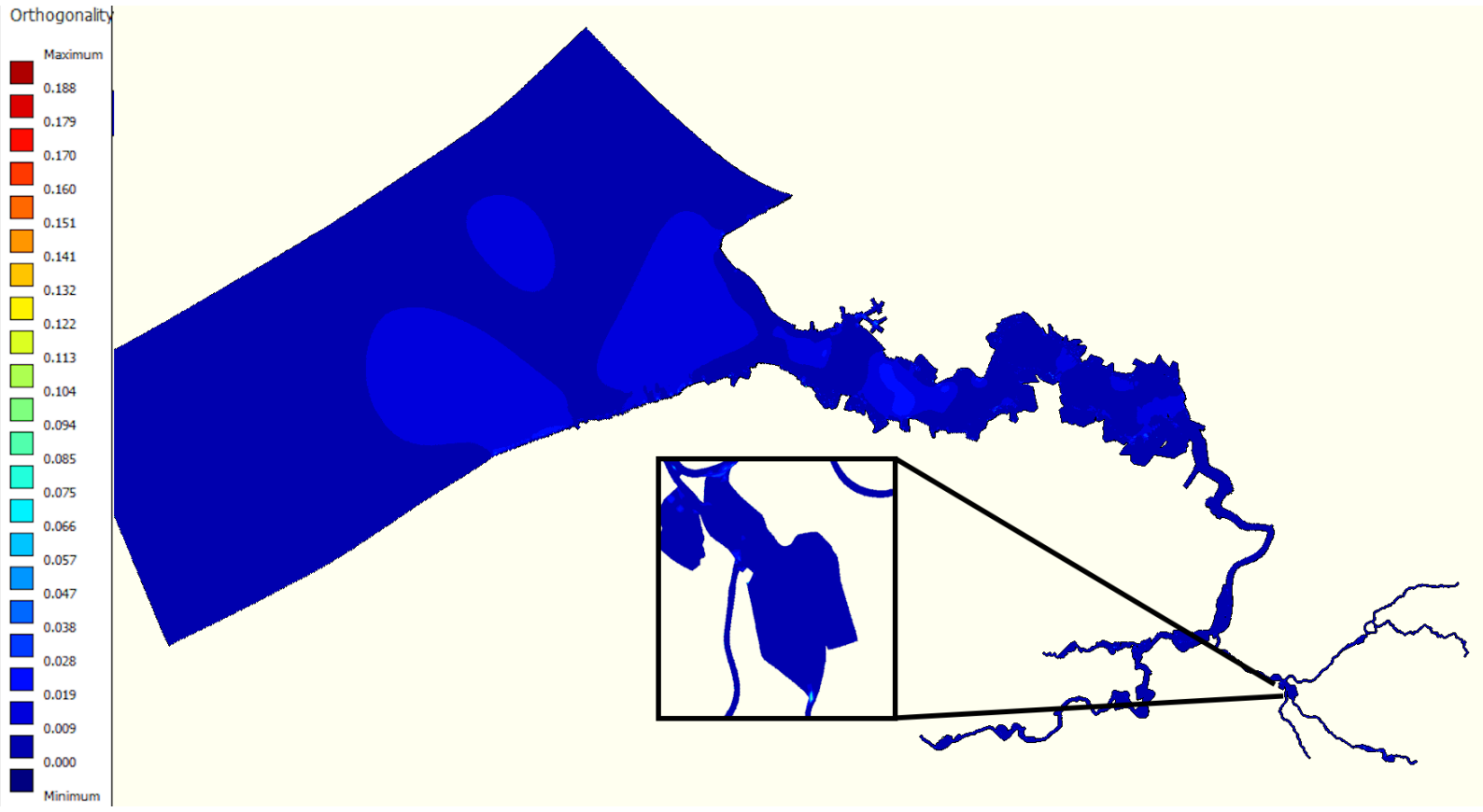

Figure 12 model orthogonality with an in zoomed part of one of the MRS

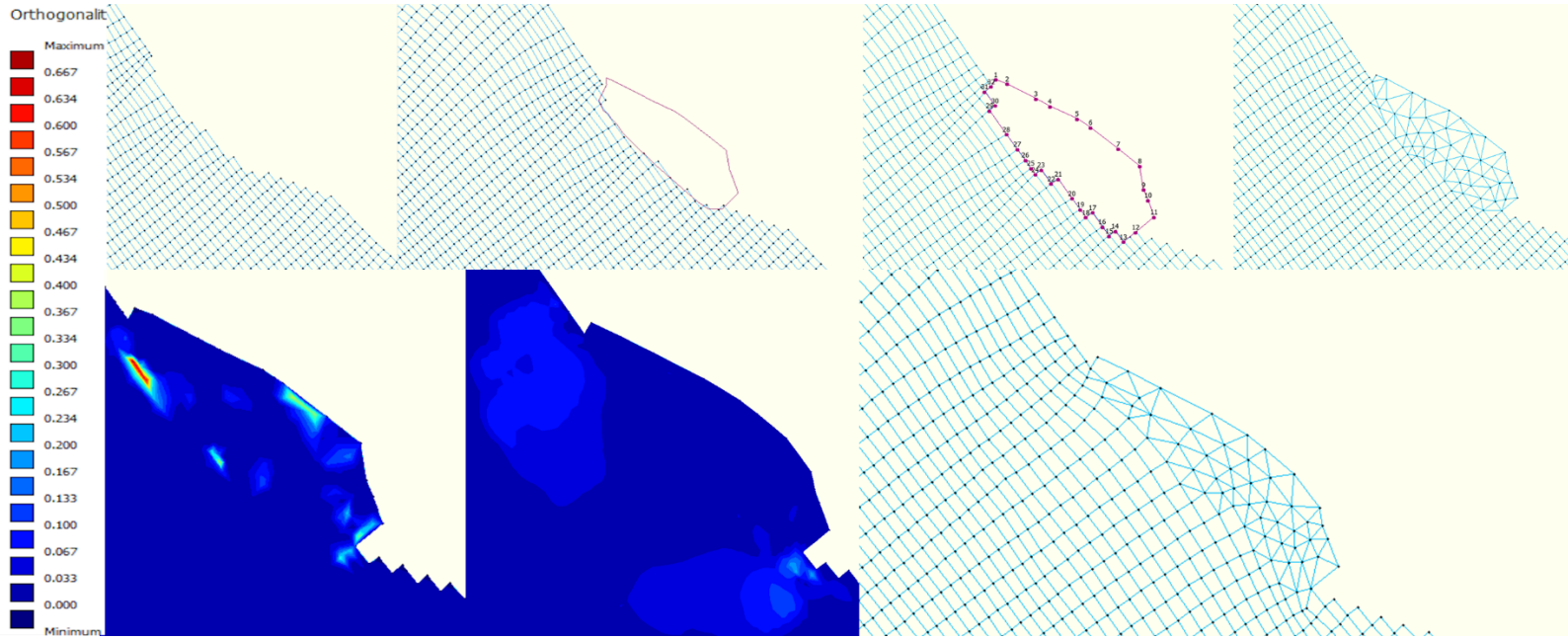

Figure 13 steps of adding MRS to orginal grid started from the upper left figure.

Furthermore, some of the MRS were either already included in the existing model or located outside the model's scope, and these areas were excluded. See Figure 14 for an example.

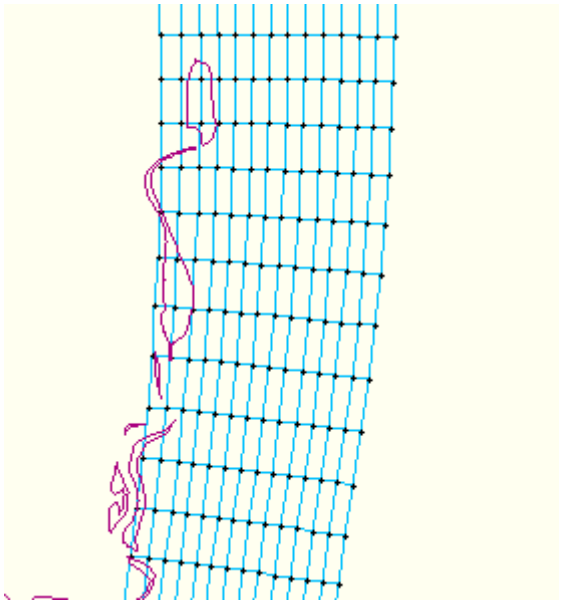

Figure 14 MRS polygons that are positioned in the original grid

To close of the MRS a thin dam is used. This creates an easy way to change the different scenarios, and it will not influence within the scenarios as much.

C. Spin up time

What

One critical challenge in process-based numerical modeling is accurately specifying the initial conditions of the estuary, as these conditions greatly affect the model's response. In this study, the required spin-up time was not known in advance. The spin-up period is an adjustment phase that allows the model to stabilize and reach an 'optimal' state, during which internal variables, such as salinity, evolve from their estimated initial conditions to this steady state. For example, a study referenced required a total of six months to fully establish a hydrodynamic model with stable conditions (Fossati & Piedra-Cueva, 2013).

Why

This paper aims to investigate the impact of MRS on salt intrusion length. It is crucial to establish that any observed changes in the results solely resulted due to the MRS attachments. To ensure this, it is essential to determine the spin-up period, after which only the MRS will influence the model's outcomes.

How

By consistently applying the same forcing over a specific period, it becomes possible to identify differences between these intervals. If no variations are observed across the different months, the model can be considered stable. For this experiment, a calm month with no storms or drought was selected to represent a typical year. June 2013 was chosen, with a period length of approximately 29.25 days, allowing the capture of two full cycles of the spring-neap tides, thereby providing a more comprehensive annual data profile due to the near-monthly repetition. A script was developed to identify the smoothest transition period between May 28, 2013, and June 30, 2013, with a duration ranging from 28 to 30 days, for all 71 forcing points at the model boundary. These points include 30 velocity measurement locations at the northern and southern boundaries along the North Sea coastline and 41 water level measurement points parallel to the coastline in the western part of the study area (see Figure 15). The discharge data for the entire year was averaged to a single value for the specific location.

Figure 15 Boundary lines of the grid with s(t) is water level/discharge and v(t) is velocity

The smoothness of the connection between forcing periods was evaluated based on both the value and the derivative at the connection points, considering the last point of the first interval and the first point of the second interval. The derivative was scaled to significantly influence the score, ensuring similar slopes and preventing sharp peaks that could disrupt the phase of the data. To balance the average score across all boundary lines, the southern velocity line, which is the most distinct with only 13 points, was weighted three times more than the others. The optimal interval was determined to be exactly 29 days, beginning on May 5, 2013, at 22:40. Figures 16, 17 and 18 shows the connection points for three arbitrary locations along the different boundary lines. A linear transition of one data step between repeated intervals was added, which proved effective for all points.

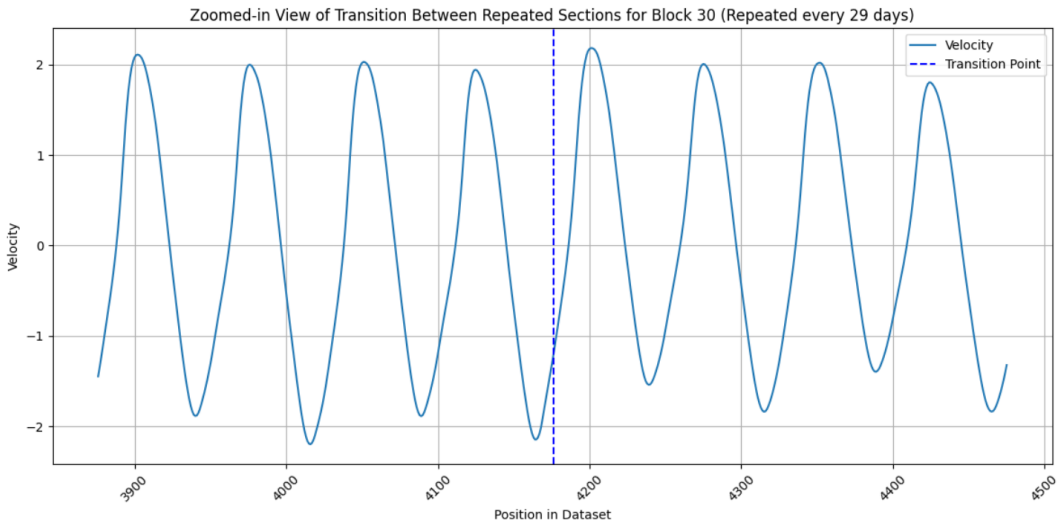

Figure 16 velocity over time graph showing the connection between the end and start data of position 30.

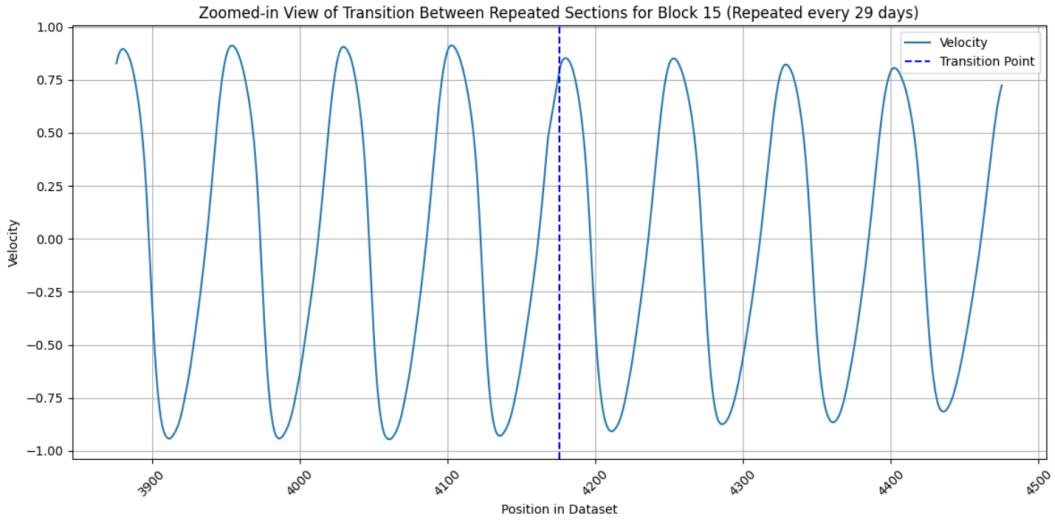

Figure 17 velocity over time graph showing the connection between the end and start data of position 15

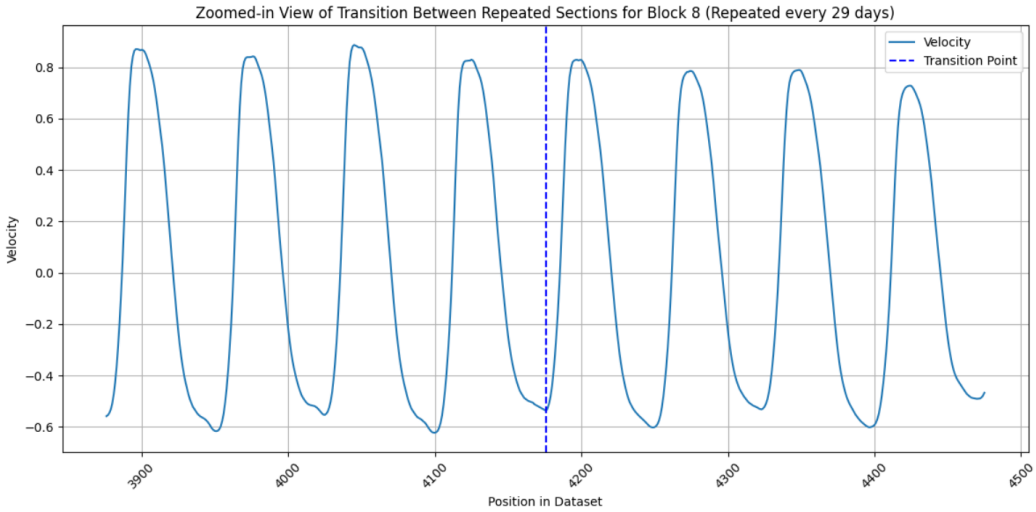

Figure 18 velocity over time graph showing the connection between the end and start data of position 8

The results of the spin up time are shown in Figure 19, the difference between the date and 29 days later for the scenario of All MRS Open. As can be seen with the trendlines the spin up period for around month 7.

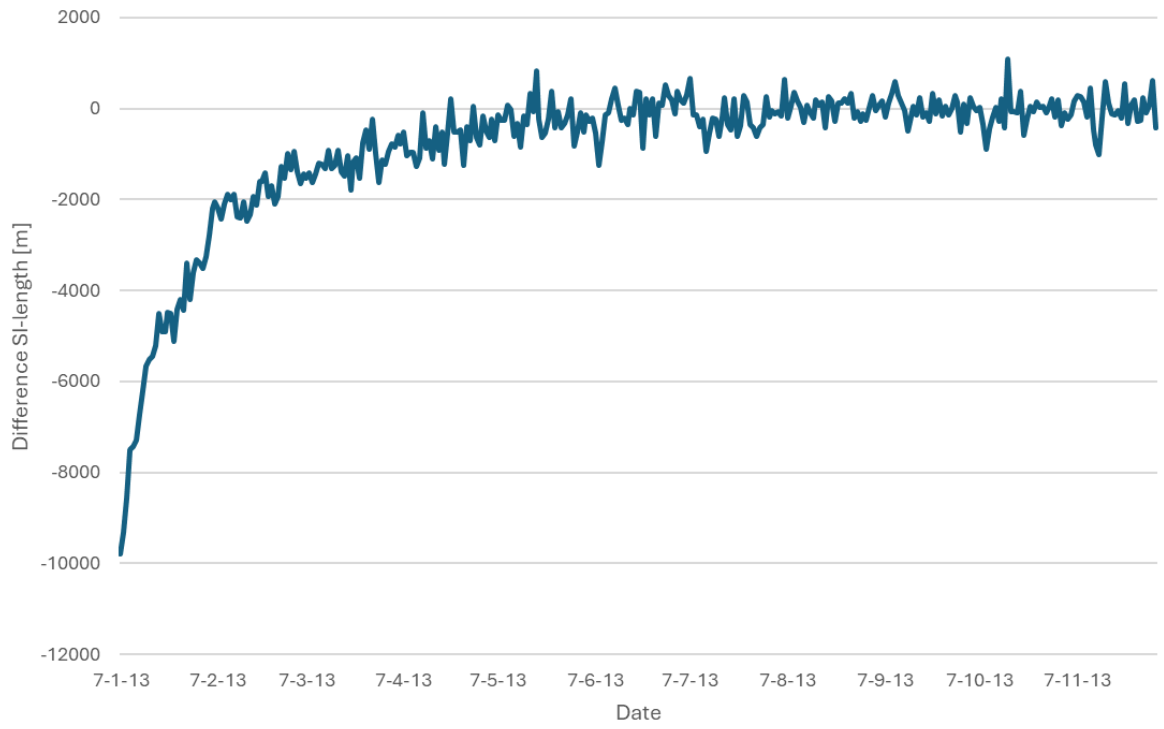

Figure 19 Delta graph of the salt intrusion length vs the salt intrusion length 29 days later for scenario All MRS Open, including an exponential trendline.